Bioorganic & Medicinal Chemistry Letters 23 (2013) 1662–1666

Contents lists available at SciVerse ScienceDirect

Bioorganic & Medicinal Chemistry Letters

journal homepage: www.elsevier.com/locate/bmcl

Structure-guided design, synthesis and in vitro evaluation of a series of pyrazole-based fatty acid binding protein (FABP) 3 ligands

Yoko Beniyama, Kenji Matsuno, Hiroyuki Miyachi *

Graduate School of Medicine, Dentistry and Pharmaceutical Sciences, Okayama University 1-1-1, Tsushima-Naka, Kita-ku, Okayama 700-8530, Japan

ARTICLE INFO

Article history:
Received 22 December 2012
Revised 11 January 2013
Accepted 16 January 2013
Available online 26 January 2013

Keywords:
Heart fatty acid binding protein
FABP3
Pyrazole
Structural design

ABSTRACT

We designed a series of pyrazole-based carboxylic acids as candidate ligands of heart fatty acid binding protein (H-FABP, or FABP3), based on a comparison of the X-ray crystallographic structures of adipocyte fatty acid binding protein (FABP4)–selective inhibitor (BMS309403) complex and FABP3–elaidic acid complex. Some of the synthesized compounds exhibited dual FABP3/4 ligand activity, and some exhibited selectivity for FABP3.

The increasing availability of three-dimensional structures of proteins and protein–ligand complexes has proved extremely helpful in allowing medicinal chemists to design ligands with increased potency and selectivity. Here, we adopted this approach with the aim of obtaining subtype-selective fatty acid-binding protein (FABP) ligands.

Cytosolic FABPs are a family of low-molecular-weight (about 14–15 kDa) proteins, expressed in a tissue-specific manner, which bind medium- to long-chain fatty acids as endogenous ligands.[1] They are involved in modulating intracellular lipid metabolism, regulation of gene expression, and intracellular shuttling of fatty acids.[2] Nine FABPs have been identified to date, that is, FABP1–9, or liver (l-), intestinal (i-), heart (h-), adipocyte (a-), epidermal (e-), ileal (il-), brain (b-), myelin (m-) and testis (t-) FABPs.[3] Although the primary sequences of the FABPs show significant diversity (15–70% sequence identity), the FABPs exhibit very similar three-dimensional structures, consisting of 10 antiparallel β-strands folded into two β-sheets, which form a β-barrel with an internal ligand-binding cavity (Fig. 2).[4] A helix-turn-helix motif serves to close the main opening to the β-barrel.

Because of the biological activities of FABPs, ligands that may modulate the functions of FABPs function are of interest. In particular, many researchers have focused on the creation of FABP4 (adipocyte FABP or aP2) inhibitors with the aim of discovering candidate drugs for the treatment of diabetes and atherosclerosis (Fig. 1).[5–7] The rationale for this is that disruption of FABP4 in mice prevents development of diet-induced insulin resistance,[8] and macrophage-specific deletion of FABP4 has a protective effect against atherosclerosis in apolipoprotein E-deficient mice.[9] However, ligands for other subtype-specific FABP ligands have received relatively little attention. Therefore, we set out to design ligands for human heart FABP (FABP3), which shows 65% sequence identity with human FABP4. The function of FABP3 is not completely disclosed, but some report indicated that FABP3 is also involved in lipid homeostasis, for FABP3 is involved in the uptake of fatty acids and their subsequent transport towards the mitochondrial β-oxidation systems.[10]

We focused on pyrazole-based FABP4-selective inhibitors **1**[11] (BMS309403) and **2**[12] as lead compounds (Fig. 1).

Compound **1** is a potent and selective FABP4 inhibitor, and the X-ray crystallographic structure of FABP4–BMS309403 complex is available in PDB (pdb: 2nnq: Fig. 2A).[11] Pyrazole derivative **2** was reported to exhibit more potent FABP4-inhibitory activity than BMS309403. On the other hand, the three-dimensional structure of FABP3–elaidic acid (a naturally occurring long-chain unsaturated fatty acid) complex is also available (pdb: 1hmr: Fig. 2C).[13] As mentioned above, the structural folds of FABP4 and FABP3 are well conserved, that is, both molecules consist of ten antiparallel β-strands folded into two β-sheets, which form a β-barrel with an internal ligand-binding cavity. BMS-309403 and elaidic acid interact with the same amino acids, which form a hydrophobic cavity, and their carboxylic acid moieties form hydrogen-bonding interactions with Arg126 and Tyr128 (FABP4 sequence). The residual hydrophobic tail part of both molecules lies in the vast hydrophobic cavity of each FABP.

In order to create ligands that preferentially bind to FABP3, we computationally introduced BMS309403 into the ligand-binding

* Corresponding author.
E-mail address: miyachi@pharm.okayama-u.ac.jp (H. Miyachi).

0960-894X/$ - see front matter © 2013 Elsevier Ltd. All rights reserved.
http://dx.doi.org/10.1016/j.bmcl.2013.01.054

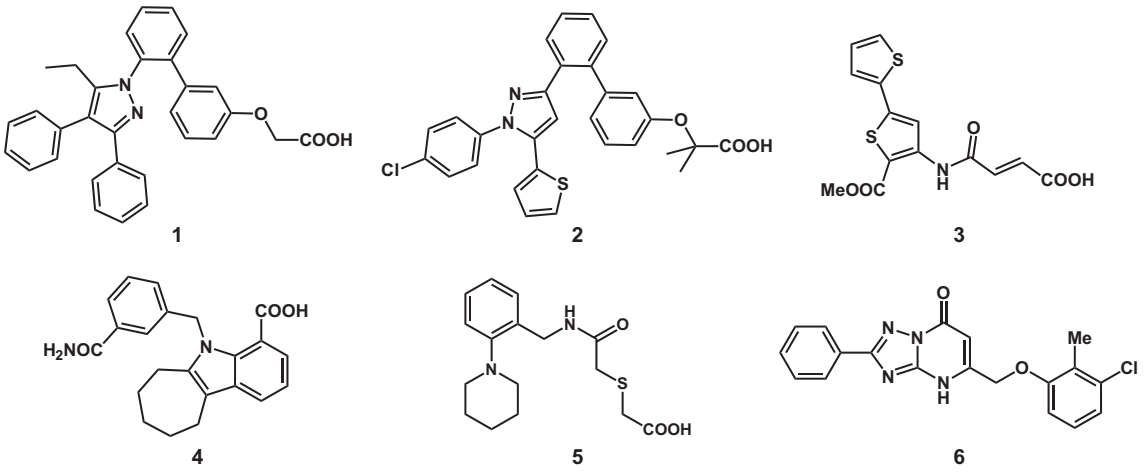

Figure 1. Representative synthetic FABP inhibitors. **1**–**4**: FABP4-selective inhibitors. **5**: FABP3/4 dual inhibitor. **6**: FABP4/5 dual inhibitor.

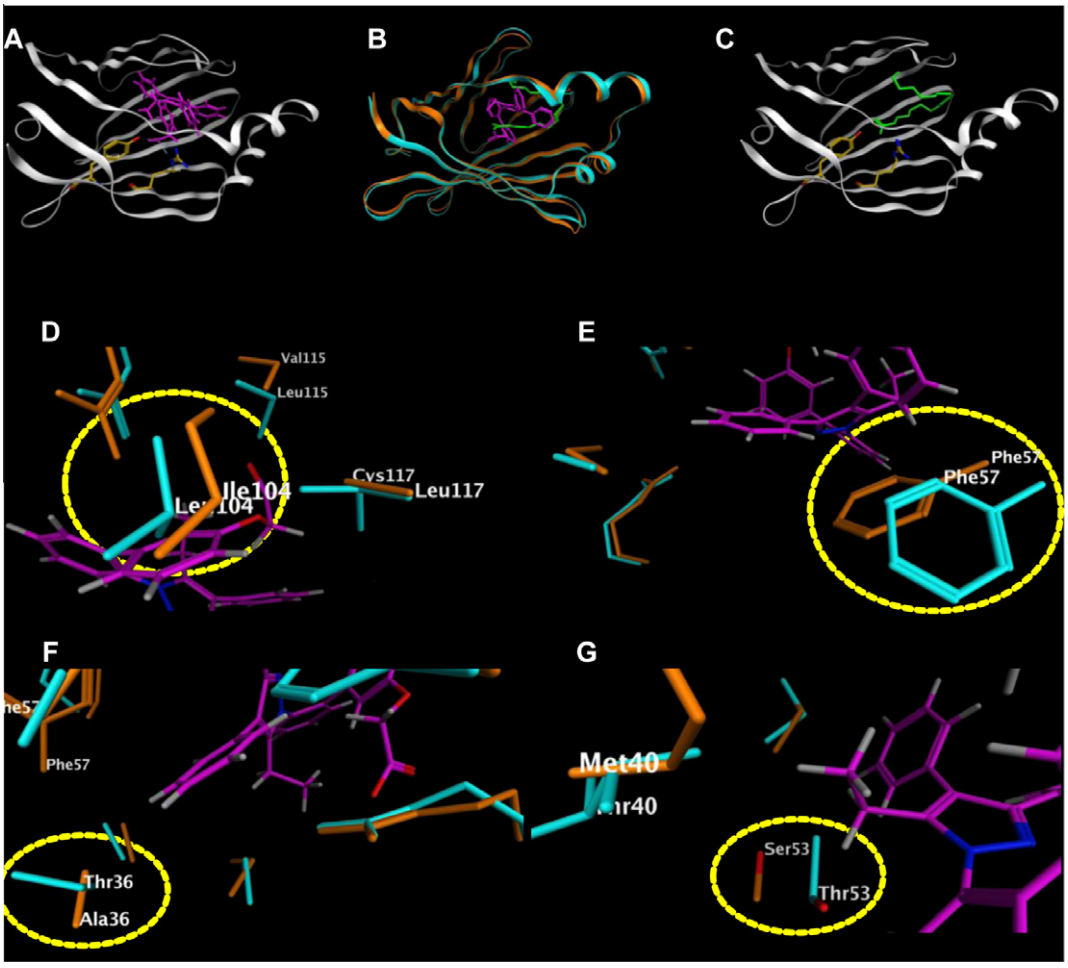

Figure 2. X-ray crystallographic structures of fatty acid binding protein (FABP)–ligand complexes and superimposed structures of FABP4 and FABP3 complexed with BMS309403. (A) FABP4–BMS309403 complex (PDB: No. 2NNQ). (B) Superimposed structure of FABP4–BMS309403 complex and FABP3–elaidic acid complex. (C) FABP3–elaidic acid complex (PDB: No. 1HMR). Amino acids located near (D) the phenoxyacetic acid part, (E) the 3-position of the pyrazole ring, (F) the 4-position of the pyrazole ring, and (G) the 5-position of the ethyl ring of BMS309403 are shown.

cavity of FABP3 in the Molecular Operating Environment, MOE (we did not take into account induced fit, for convenience). The results are depicted in Figure 2D–G.

We noted that the proximal phenyl group of the biphenyloxyacetic acid moiety of BMS-309403 interacted with the small binding cavity of FABP4, formed from Tyr19, Glu72, His93, Glu95, Ile104, Arg106 and Cys117. However the corresponding amino acid 104 of FABP3 is Leu instead of Ile. The side-chain isobutyl group of Leu104 appears to have a short contact with the benzene ring of the biphenyloxyacetic acid moiety of BMS309403. Therefore the

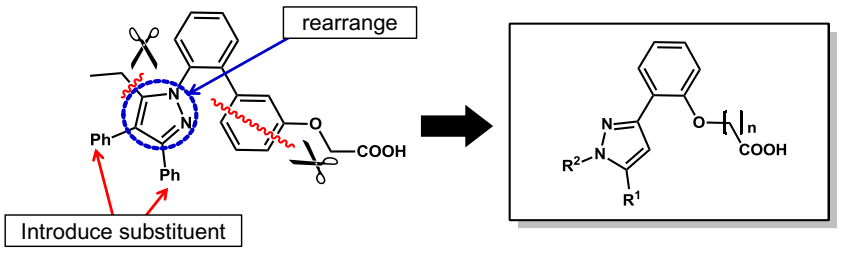

Figure 3. General formula of the present series of FABP3 ligands based on FABP4-selective inhibitor BMS-309403 as a template.

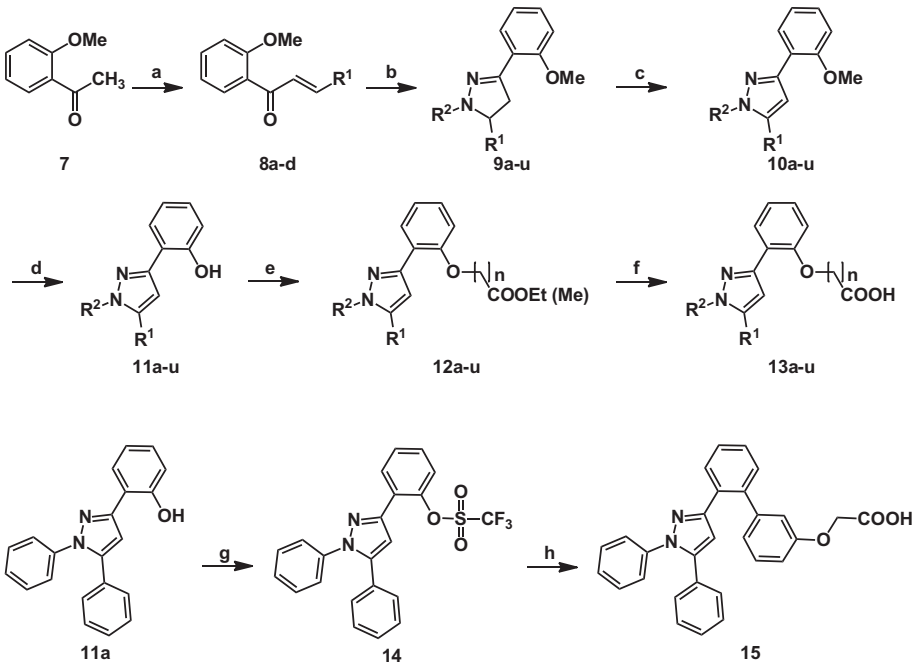

Scheme 1. Synthesis of 1,3,5-trisubstituted pyrazole derivatives. Reagents and conditions: (a) benzaldehyde derivatives, 10% KOH, EtOH, rt, 2 days, 78–96%; (b) phenylhydrazine HCl derivative (or cycloalkylhydrazine HCl derivative), EtOH, reflux, 20 h, 43–87%; (C) DDQ, benzene, reflux, 16 h, 63–94%; (d) BBr_3, dry CH_2Cl_2, −78 to 0 °C, 7 h, 47–97%; (e) Br-$(CH_2)n$-CO_2R (R = Me or Et)), NaH, dry DMF, 0–50 °C, 4 h, 47–91%; (f) 1 mol/L NaOH, EtOH, 50 °C, 4 h, 35–97%; (g) trifluoromethanesulfonic anhydride, pyridine, dry CH_2CL_2, 0–20 °C, 4 h, 98%; (h) (1) ethyl 2-(3-(4,4,5,5-tetramethyl-1,3,2-dioxaborolan-2-yl)phenoxy)acetate, Cs_2CO_3, $Pd(OAc)_2$, BINAP, 1,4-dioxane, reflux, overnight, 46% (2) 1 mol/L NaOH, MeOH, 50 °C, 3 h, 86%.

presence of this proximal phenyl group attached at the 1-position nitrogen atom of the pyrazole nucleus might be unfavorable for a FABP3 selective ligand (Fig. 2D). The phenyl group at the 3-position of the pyrazole ring of BMS309403 interacted with the small binding cavity of FABP4, formed from Phe16, Met20, Val25, Ala33, Phe57, Ala75, Asp76 and Arg78, but the side-chain benzyl group of the corresponding Phe57 of FABP3 is located far distant (Fig. 2E). Also, the phenyl group attached at the 4-position of the pyrazole ring of BMS309403 interacted with the side chain amino acids of Phe16, Ala33, Ala36 Pro38, Ser55, Phe57 and Arg126 of FABP4. However the corresponding amino acid 36 of FABP3 is Thr instead of Ala. As a consequence, the hydrophobic pocket hosting the 4-phenyl group of the pyrazole ring of BMS309403 is wider in the case of FABP3 (Fig. 2F). These structural differences prompted us to speculate that the introduction of suitable substituent(s) at the phenyl groups on the pyrazole ring of BMS309403 might selectively increase the affinity for FABP3. Finally, the ethyl group at the 5-position of the pyrazole ring of BMS309403 interacted with a small 'dimple' composed of the side chain amino acids of Pro38, Asn39, Met40, Ser53 and Tyr128 of FABP4. But, in the case of FABP3, the corresponding amino acids 40 and 53 of FABP3 are Thr and Thr instead of Ser and Met. Notably, Thr53 is located close to the methylene group of the 5-position ethyl group. Therefore, the presence of this ethyl group might be unfavorable for FABP3-selecive ligands (Fig. 2G). Based on these structural considerations, we focused on the general formula depicted in Figure 3 as a putatively selective ligand structure for FABP3.

The synthetic route to the present series of designed compounds is shown in Scheme 1. Condensation of chalcone derivatives, prepared from the aldol condensation of 2-methoxyacetophenone and substituted benzaldehydes with substituted phenylhydrazines HCl (or cycloalkylhydrazines HCl) under acidic conditions in ethanol yielded tri-aromatic substituted 4,5-dihydro-1*H*-pyrazoles **9a–u**, which were aromatized to pyrazoles **10a–u** by means of 2,3-dichloro-5,6-dicyano-1,4-benzoquinone (DDQ) oxidization.[14] As previously reported, when the cyclization reaction was performed in DMSO as a solvent, cyclization and subsequent aromatization occurred to form the pyrazole ring,[14] but in poor yield, and the product was impure. The methoxy group was demethylated with BBr_3, alkylated with ethyl (or methyl) bromo alkanoate, and hydrolyzed with alkali to afford the desired compounds **13a–u**. Biphenyloxyacetic acid type compound **15** was also prepared for comparison.

All compounds were tested for binding-inhibitory activity in the 8-anilino-1-naphthalenesulfonic acid (1,8-ANS)-based fluores-

Table 1
FABP-inhibitory activities of the present series of compounds

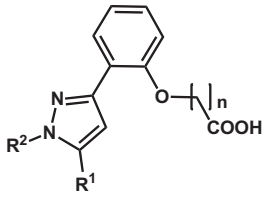

No.	R^1	R^2	n	IC_{50} (μM)	
				FABP 3	FABP 4
13a	4-ClPh	Ph	1	>10,000	>10,000
13b	4-ClPh	Ph	3	21.0	6.13
13c	4-ClPh	Ph	4	243	74.0
13d	4-ClPh	Ph	6	>10,000	31.0
13e	4-MePh	Ph	3	4730	5.41
13f	4-BrPh	Ph	3	224	9.51
13g	Ph	Ph	3	2.18	3.02
13h	Ph	Ph	4	>10,000	6.39
13i	4-MePh	Ph	4	>10,000	259
13j	4-BrPh	Ph	4	22.3	86.0
13k	Ph	4-FPh	3	2.01	10.2
13l	Ph	4-BrPh	3	0.733	5.64
13m	Ph	4-ClPh	3	0.748	4.32
13n	Ph	4-*i*PrPh	3	0.787	10.3
13o	Ph	4-MeOPh	3	1.65	13.6
13p	Ph	2-ClPh	3	1.16	4.27
13q	Ph	2-MeOPh	3	505	IA
13r	Ph	3-ClPh	3	0.695	2.50
13s	Ph	Cyclopentyl	3	6.03	16.6
13t	Ph	Cyclohexyl	3	5.26	23.5
13u	Ph	Cycloheptyl	3	6.47	15.5
1				14.7	0.221
15				>10,000	0.987

Data are the mean of two duplicated independent assay results.

cence displacement assay developed by Kane and Bernlohr,[15] with a slight modification (all the test compounds were dissolved in ethanol instead of DMSO, for DMSO decreased fluorescent intensity). The results, expressed as IC_{50} (μM), are summarized in Table 1. BMS309403 was utilized as the positive control to validate the screening assay. In our assay system, BMS309403 exhibited a sub-micromolar IC_{50} value towards FABP4, with more than 50-fold selectivity over FABP3,[15] in agreement with reported data.

Although we did not find a clear-cut structure–activity relationship, some important features were noted. Compound **15**, a positional isomer of BMS309403 lacking the ethyl side chain, exhibited a somewhat decreased, but still potent, IC_{50} value against FABP4, as compared with BMS309403. But, it did not inhibit FABP3 activity at the highest concentration of 10,000 μM, so its FABP4 selectivity is superior to that of BMS-309403. Alkyl tether length, connecting the carboxyl group and the phenolic oxygen, strikingly affected activity towards both FABPs. In the case of FABP3, the acetic acid derivative (**13a**: $n = 1$), was ineffective even at the highest concentration examined. The butyric acid derivative (**13b**: $n = 3$), showed comparable inhibitory activity towards both FABP's, while the pentanoic acid derivative (**13c**: $n = 4$) exhibited decreased inhibitory activity as compared with **13b**. Therefore, we selected the tether length of $n = 3$.

We next turned our attention to the R^1 position. Introduction of a 4-position substituent at the R^1 phenyl group greatly affected FABP3-inhibitory activity, that is, the 4-methyl and 4-bromo derivatives, **13e** and **13f**, exhibited reduced FABP3-inhibitory activity, whereas the unsubstituted phenyl derivative, **13g**, retained the activity. As for FABP4, these compounds exhibited comparable micromolar-order inhibitory activity. These results indicate that the introduction of a 4-position substituent did not greatly affect the FABP4-inhibitory activity, suggesting that there is a difference between the modes of interaction with FABP3 and FABP4. We

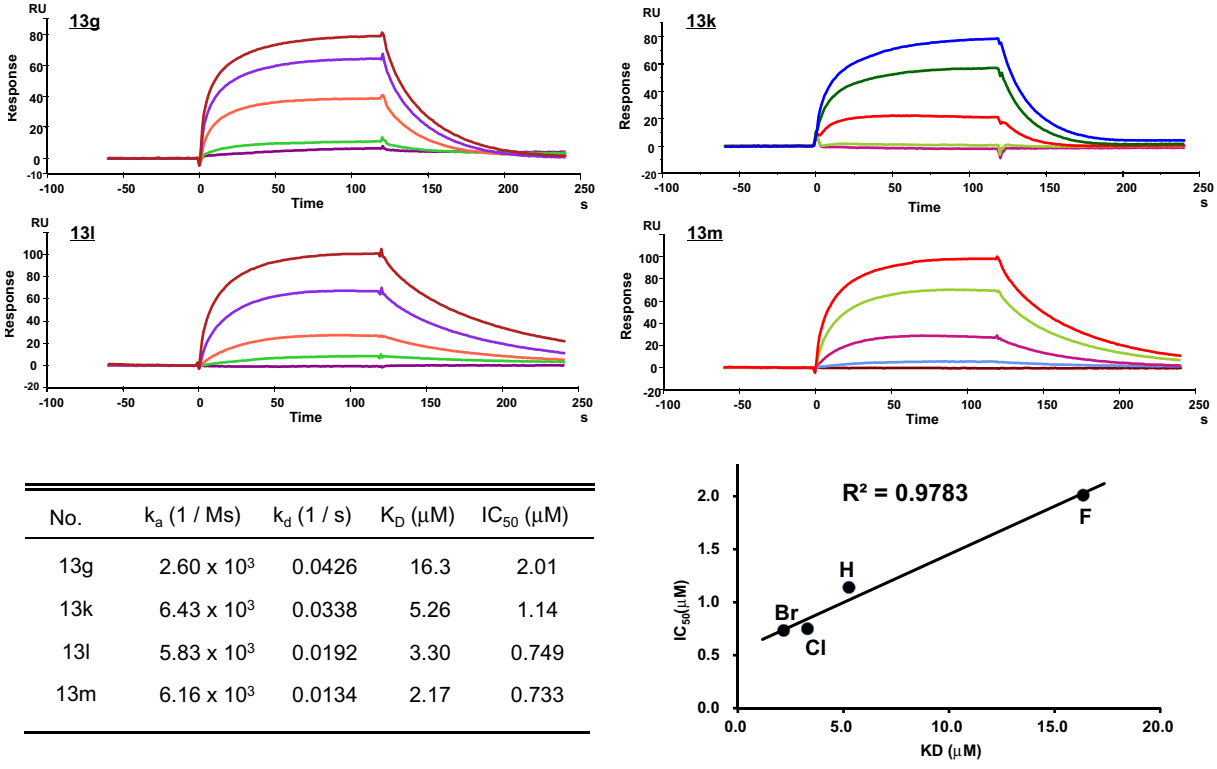

No.	k_a (1 / Ms)	k_d (1 / s)	K_D (μM)	IC_{50} (μM)
13g	2.60 x 10^3	0.0426	16.3	2.01
13k	6.43 x 10^3	0.0338	5.26	1.14
13l	5.83 x 10^3	0.0192	3.30	0.749
13m	6.16 x 10^3	0.0134	2.17	0.733

Figure 4. Representative Biacore sensorgrams, using FABP3-functionalized CM5 sensors, together with physico-chemical parameters, and the correlation between KD and IC_{50} values.

selected the unsubstituted phenyl group as the optimum R^1 substituent.

Then we moved on to the R^2 substituent. It is noteworthy that the effect of a substituent introduced at the 4-position of the benzene ring is small as compared to the case of the R^1 substituent. Compounds **13k–13o** exhibited micromolar to sub-micromolar order IC_{50} values towards FABP3. Change of the position of the substituent from the 4-position to the 2- or 3-position might be tolerable in the case of a relatively small chlorine atom. However, the 2-MeO derivative **13q** exhibited decreased FABP3-inhibitory activity. Similar tendencies were also seen in the case of FABP4, though the activities were rather weak. As a R^2 substituent, an aromatic ring is preferable to a cycloalkyl ring, because all three cycloalkyl ring derivatives **13s–13u** exhibited decreased inhibitory activities towards both FABPs. In the present series, compounds **13l**, **13m** and **13n** exhibited selective FABP3-inhibitory activity at submicromolar concentration.

In order to confirm that the FABP3-inhibitory activities of the present series of compounds were due to direct binding of the compounds to FABP3, we performed direct binding assay of representative compounds (**13g**, **13k–13m**) based on the principle of the surface plasmon resonance, using a Biacore X 100 system with a FABP3-functionalized sensor-chip (Fig. 4). We observed micromolar-order KD values, ranging from 2 to 16 μM, which were well correlated with the IC_{50} values ($R^2 = 0.98$). These data clearly indicated that the pyrazole compounds directly bind to the binding pocket of FABP3, and compete with the fluorescent ligand 1, 8-ANS.

In conclusion, we designed and synthesized a series of 1,3,5-trisubstituted pyrazole derivatives as candidate FABP3 ligands, and found that 4-(2-(1,5-diphenyl-1*H*-pyrazol-3-yl)phenoxy)butanoic acid structure is a good lead structure for FABP3-selective inhibitors. Further structural development and in vitro pharmacological evaluation of the present series of compounds are under way.

Acknowledgments

We thank Drs. Takaaki Miyaji and Asako Kawakami for Biacore binding analyses.

This work was supported in part by the Drug Discovery for Intractable Infectious Diseases Project, Graduate School of Medicine, Dentistry and Pharmaceutical Sciences, Okayama University, the Uehara Memorial Foundation, the Tokyo Biochemical Research Foundation (TBRF), and the Okayama Foundation for Science and Technology (OFST).

References and notes

1. Owada, Y. *Tohoku J. Exp. Med.* **2008**, *214*, 213.
2. Storch, J.; Corsico, B. *Annu. Rev. Nutr.* **2008**, *28*, 73.
3. Furuhashi, M.; Hotamisligil, G. S. *Nat. Rev. Drug Disc.* **2008**, *7*, 489.
4. (a) Storch, J.; Thumser, A. E. *J. Biol. Chem.* **2010**, *285*, 32679; (b) Banaszak, L.; Winter, N.; Xu, Z.; Bernlohr, D. A.; Cowan, S.; Jones, T. A. *Adv. Protein Chem.* **1994**, *45*, 89.
5. Cai, H.; Yan, G.; Zhang, X.; Gorbenko, O.; Wang, H.; Zhu, W. *Bioorg. Med. Chem. Lett.* **2010**, *20*, 3675.
6. Ringom, R.; Axen, E.; Uppenberg, J.; Lundbäck, T.; Rondahl, L.; Barf, T. *Bioorg. Med. Chem. Lett.* **2004**, *14*, 4449.
7. Barf, T.; Lehmann, F.; Hammer, K.; Haile, S.; Axen, E.; Medina, C.; Uppenberg, J.; Svensson, S.; Rondahl, L.; Lundbäck, T. *Bioorg. Med. Chem. Lett.* **2009**, *19*, 1745.
8. Tilg, H.; Moschen, A. R. *Mol. Med.* **2008**, *14*, 222.
9. Holm, S.; Ueland, T.; Dahl, T. B.; Michelsen, A. E.; Skjelland, M.; Russell, D.; Nymo, S. H.; Krohg-Sørensen, K.; Clausen, O. P.; Atar, D.; Januzzi, J. L.; Aukrust, P.; Jensen, J. K.; Halvorsen, B. *PLoS One* **2011**, *6*, e28785.
10. Veerkamp, J. H.; Moerkerk, H. T. *Mol. Cell. Biochem.* **1993**, *123*, 101.
11. Sulsky, R.; Magnin, D. R.; Huang, Y.; Simpkins, L.; Taunk, P.; Patel, M.; Zhu, Y.; Stouch, T. R.; Bassolino-Klimas, D.; Parker, R.; Harrity, T.; Stoffel, R.; Taylor, D. S.; Lavoie, T. B.; Kish, K.; Jacobson, B. L.; Sheriff, S.; Adam, L. P.; Ewing, W. R.; Robl, J. A. *Bioorg. Med. Chem. Lett.* **2007**, *17*, 511.
12. Liu, X.; Huang, X.; Lin, W.; Wang, D.; Diao, Y.; Li, H.; Hui, X.; Wang, Y.; Xu, A.; Wu, D.; Ke, D. *Bioorg. Med. Chem. Lett.* **2011**, *21*, 2949.
13. Young, A. C.; Scapin, G.; Kromminga, A.; Patel, S. B.; Veerkamp, J. H.; Sacchettini, J. C. *Structure* **1994**, *2*, 523.
14. Huang, Y. R.; Katzenellenbogen, J. A. *Org. Lett.* **2000**, *2*, 2833.
15. Kane, C. D.; Bernlohr, D. A. *Anal. Biochem.* **1996**, *233*, 197.